Microchim Acta (2017) 184:1977–1985
DOI 10.1007/s00604-017-2175-6

ORIGINAL PAPER

Voltammetric sensor for trichloroacetic acid using a glassy carbon electrode modified with Au@Ag nanorods and hemoglobin

Dongping Qian[1] · Weibo Li[1] · Fangting Chen[1] · Ying Huang[1] · Ning Bao[1] · Haiying Gu[1] · Chunmei Yu[1]

Received: 12 October 2016 / Accepted: 8 March 2017 / Published online: 30 March 2017

Abstract Core-shell Au@Ag nanorods (Ag@GNRs) were synthesized and utilized to construct a voltammetric biosensor for trichloroacetic acid (TCA). The biosensor was prepared by immobilizing hemoglobin (Hb) on a glassy carbon electrode (GCE) that was modified with the Ag@GNRs. Cyclic voltammetry revealed a pair of symmetric redox peaks, indicating that direct electron transfer occurs at the Hb on the Ag@GNR-film. The electron transfer rate constant is as high as 2.32 s^{-1}. The good electrocatalytic capability and large surface area of the Ag@GNR-film is beneficial in terms of electron transfer between Hb and the underlying electrode. The modified GCE, best operated at −0.4 V (vs. SCE), exhibits electrocatalytic activity toward TCA in the 0.16 μM to 1.7 μM concentration range, with a 0.12 μM detection limit (at an S/N ratio of 3).

Keywords Core-shell nanorods · Self-assembly · Electrocatalysis · Amperometry · Biosensor · Laviron equation

Introduction

Hemoglobin (Hb) is a tetrameric heme protein comprised of two α chains and two β chains [1]. Hb can be used as an ideal model molecule for the research of the redox of proteins and biological sensing due to its relatively stable structure. However, it is difficult to obtain effective electrochemical signals and study the electrochemical behavior of Hb at the bare electrode surface due to its relatively large spatial structure and electroactive center is hard to expose. In addition, the adsorption of Hb on the bare electrode may lead to the passivation of electrode and the restriction of electron transfer rates [2]. Therefore, researchers have tried to modify electrodes using different kinds of nanomaterials such as graphene [3], quantum dots [4], metal nanoparticles [5], etc. to achieve its direct electrochemistry.

Among various shapes of gold nanoparticles (GNPs), gold nanorods (GNRs) attracted substantial attention [6, 7]. In addition to the unique optical properties [8], GNRs possess general properties similar to GNPs such as better conductivity, and have several advantages over the spherical GNPs, including fast electron transfer rate and high surface area [9, 10], which inspire researchers to explore the application of GNRs in electrochemical biosensors [11, 12]. Nevertheless, GNRs are prone to agglomeration which causes a loss of its own features. Therefore, the core-shell Au@Ag nanorods (Ag@GNRs) have attracted much attention due to their tunability in nanometer-scale structure and tunable longitudinal SPR peaks as well as chemical stabilities [13, 14] Combined with the superior catalytic activity of Au and Ag, Ag@GNRs have been synthesized and utilized in dopamine detection [15], genes analysis [16] and electrochemical immunoassay [17].

Trichloroacetic acid (TCA) is a class of environmental contaminants which has certain carcinogenic and caused serious impact on human life [18]. It can be found not only in the industrial waste water but also in drinking water as disinfection by-product [19]. Therefore, it is of great significance for developing a simple, rapid, selective and sensitive method to

Electronic supplementary material The online version of this article (doi:10.1007/s00604-017-2175-6) contains supplementary material, which is available to authorized users.

✉ Haiying Gu
hygu@ntu.edu.cn

✉ Chunmei Yu
cmyu@ntu.edu.cn

[1] School of Public Health, Nantong University, Nantong 226019, People's Republic of China

detect TCA. There are many methods for the detection of TCA such as gas chromatography [20], high performance liquid chromatography [21] and mass spectrometry [22]. These methods with adequate sensitivity are difficult for in-situ or online monitoring and suffered from expensive equipments, time-consuming for procedures of derivation and extraction [23]. On the contrary, electrochemical sensor shows its advantages over these drawbacks owning to their intrinsic advantages such as simple operation, high sensitivity, selectivity, low cost, and good portability [24, 25]. Meanwhile, bioelectrochemically reductive TCA by Hb has been considered as a promising way for the TCA determination because it exhibits a relatively high current efficiency. Since electron transfer occurs between Hb and TCA, the activity of active centers in Hb immobilized on the electrode surface plays the key factor during the reaction process. Different kinds of Hb modified electrodes have been fabricated to investigate the electrocatalytic effect toward TCA [26–29].

In this work, Ag@GNRs have been prepared and characterized by UV-vis spectroscopy, transmission electron microscopy. Then it was used to immobilize Hb on the modified electrode surface by self-assembly technique. The synthesized Ag@GNRs can provide large surface area, superior conductivity and favorable microenvironment for retaining the biological activity of the adsorbed Hb and facilitate the direct electron transfer between the Hb and the electrode. The electrocatalytic reduction of TCA has been investigated, showing possible potential application of Ag@GNRs for the construction of biosensors.

Experimental

Reagents and materials

Bovine Hb (Hb ~ 90%, MW = 66,000), poly (diallyldimethylammonium chloride) (PDDA, 20% (m:m)), polystyrene sulfonate (PSS, MW = 70,000), sodium citrate and trichloroacetic acid (TCA) were purchased from Sigma-Aldrich (http://www.sigmaaldrich.com/). Chloroauric acid ($AuCl_3 \cdot HCl \cdot 4H_2O$) and H_2O_2 (30% (m:m)) were purchased from Sinopharm Chemical Reagent Co., Ltd. (Shanghai, China, http://www.sinoreagent.com/). Cetyltrimethyl ammonium bromide (CTAB), silver nitrate ($AgNO_3$), sodium borohydride ($NaBH_4$), ascorbic acid (AA) and sodium oleate (NaOL) were all purchased from Nantong Chengji Chemical Trade Co., Ltd. (Nantong, China, http://cjhgmy.chinapyp.com/). Solutions of H_2O_2 were prepared by dilution of H_2O_2 appropriately. Phosphate buffer (0.1 M) with different pH values were prepared by mixing stock solutions of Na_2HPO_4 and NaH_2PO_4 and adjusting the pH value with 0.1 M H_3PO_4 or NaOH solution. All other chemicals used were of analytical reagent grade. All the solutions were prepared using double distilled water.

Apparatus and methods

All electrochemical experiments were carried out on a CHI660C electrochemical workstation employing a conventional three-electrode cell. The working electrode was the modified glassy carbon electrode (GCE) (3 mm in diameter). A saturated calomel electrode (SCE) and a platinum wire electrode served as the reference electrode and the counter electrode, respectively. All electrochemical measurements were carried out under a high-purified nitrogen atmosphere. The electrolyte was 0.1 M phosphate buffer which must be purged with nitrogen for at least 20 min. The GNRs and Ag@GNRs were characterized by transmission electron microscopy (TEM) (Tecnai-12, Netherlands). UV–vis spectrum was recorded on a UV–2450 spectrophotometer (Shimadzu, Japan). Electrochemical impedance spectroscopy (EIS) was performed with an AUTOLAB PGSTAT 302 N electrochemical workstation (Metrohm, Swiss) in 0.1 M KNO_3 solution containing 1.0 mM $Fe(CN)_6^{3-}/Fe(CN)_6^{4-}$ (1:1) across the frequency range from 10^{-3} to 10^5 Hz.

Preparation of Ag nanoparticles (AgNPs), GNRs and Ag@GNRs

GNRs were chemically synthesized using seed mediated growth method [30]. Seed solution was prepared by firstly mixing 5 mL $HAuCl_4$ (0.5 mM) with 5 mL CTAB (0.2 M) and then adding 0.6 mL ice-cold $NaBH_4$ (0.01 M) under vigorous stirring. After 2 min of reaction, the prepared seeds were stored at room temperature for 30 min before use.

For the preparation of growth solution [6, 31], CTAB (9.0 g) and NaOL (1.234 g) were added to an Erlenmeyer flask and dissolved in doubly distilled water (250 mL) at 50 °C. $AgNO_3$ (12 mL, 4 mM) and $HAuCl_4$ (250 mL, 1 mM) were added to this solution when it was cooled to 30 °C. After 15 min, the mixture was stirred at 700 rpm for 90 min until it gradually became colorless and the pH was adjusted by adding 2.1 mL of 12.1 M HCl (37% (m:m)). After stirring gently at 400 rpm for 15 min, AA (1.25 mL, 0.064 M) was added to the colorless solution under stirring for 30 s. Thereafter, 0.8 mL of the seed solution was quickly added to the above solution. The resultant mixture was stirred for 30 s and left undisturbed at 30 °C for 12 h. Finally, the excess CTAB in the solution was removed by centrifugation thrice at 7000 rpm (7669 rcf) for 30 min. The GNR-solution was obtained by diluting the sediment to 10 mL with doubly distilled water.

The Ag@GNR-nanocomposite was obtained by reduction of Ag^+ on the surface of GNRs [32, 33]. $AgNO_3$ (200 μL, 10 mM) was added into the prepared GNR-solution (5 mL).

The mixture was mixed with AA (200 μL, 100 mM) and stirred for 10 min, after that, the reduction processes was finished and Ag@GNR-solution can be obtained.

For the preparation of AgNPs, a solution of 1 mM $AgNO_3$ (100 mL) was added and heated with vigorous stirring. Upon boiling, 1 mL of 10 mg·mL^{-1} sodium citrate solution was added rapidly. Then the solution was heated under reflux for approximately 1 h. Before use, it was stored at 4 °C.

Preparation of the modified electrode

Prior to modification, the GCE was firstly polished with abrasive paper and then with alumina slurry to a mirror. After being thoroughly rinsed with doubly distilled water, the well-polished GCE was cleaned in absolute ethanol by sonication. The electrode was washed with doubly distilled water and then dried in air. The GCE was dipped in turn into PDDA solution (1% (m:m)), PSS solution (2.0 mg·mL^{-1}) and Ag@GNR stock solution at 4 °C for 30 min, respectively. At last the electrode was dipped into 3.0 mg·mL^{-1} Hb solution (pH 9.0 phosphate buffer) at 4 °C for 30 min. The electrode is denoted as Hb-Ag@GNR-PSS-PDDA/GCE in abbreviation. For comparison, Hb-AgNP-PSS-PDDA/GCE and Hb-GNR-PSS-PDDA/GCE were fabricated with similar procedure.

Results and discussion

Choice of materials

With the development of nanotechnology, numerous novel nanomaterials especially noble metal nanomaterials have been extensively applied in the field of biosensor. Pure silver and gold nanoparticles, with the advantages of large specific surface area, excellent stability as well as the ability of modulating the electron transfer, have been utilized to realize the direct electron transfer of redox proteins and enzymes [34, 35]. Although the individual nanoparticles show unique shape- and size-dependent physicochemical properties, the shell-core structures, assembled from them, may give rise to some unexpected mechanical, electrical, and catalytic performances, which can be stimulated a variety of potential applications in photoelectricity, catalysis and biosensor [36, 37]. The preparation of bimetallic Ag@GNRs has attracted much attention due to their characteristic properties differ from those of the GNRs [38, 39]. The protective layer of Ag shell can not only prevent the GNRs from aggregation but also provide a better platform for further functionalization. Accordingly, considering the excellent catalytic activity of GNRs and Ag, Ag@GNRs were synthesized in this work and further applied as a function interface for Hb immobilization.

Characterization of GNRs and Ag@GNRs

TEM and UV–vis absorption spectra were used to characterize the synthesized GNRs and Ag@GNRs (Fig. 1). The average length and the aspect ratio of the GNRs are ~50 nm and ~5.1, respectively (Fig. 1a). The TEM image (Fig. 1b) reveals the morphology of Ag@GNRs, where each GNR is encircled distinctly with a layer of Ag halo. GNRs and Ag@GNRs were further confirmed by the UV–vis absorption spectra (Fig. 1c). The UV–vis absorption spectrum of GNRs exhibit two distinct absorption peaks at 509 nm and 960 nm, which are assigned to the typical transverse and longitudinal absorption peaks of GNRs, respectively. As the Ag is coated on the surface of GNRs, the longitudinal absorption peak blue shifts to 797 nm and the transverse absorption peak splits into two absorption peak bands which are the typical absorption spectrum bands of Ag@GNRs and located at 406 nm (a) and 476 nm (b), respectively. These results reveal that Ag has been wrapped on the surface of GNRs successfully.

Characterization of the modified electrode

EIS is often used to monitor the assembly process. In EIS, the semicircle part at higher frequencies corresponds to the electron-transfer limited process. Its diameter equals the electron transfer resistance, R_{et}, which exhibits the electron transfer kinetics of the redox probe at the electrode interface. Fig. S1 displays the EIS observed upon the changes of surface-modified process. The result discussed in Electronic Supplementary Material (ESM) shows that Hb has been successfully immobilized on the modified electrode.

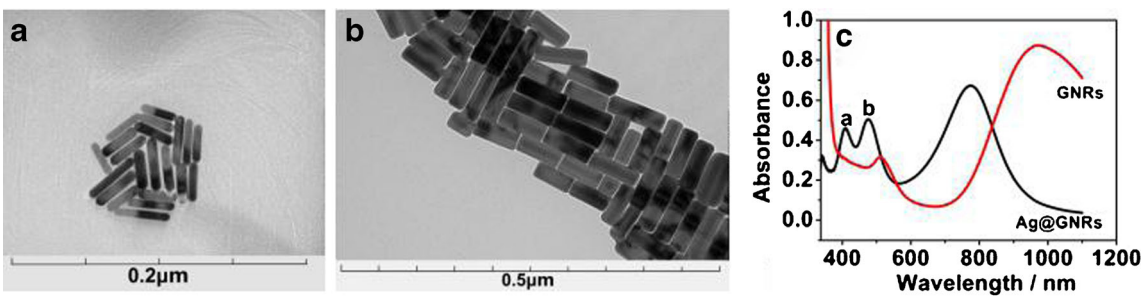

Fig. 1 TEM spectra of **a** GNRs and **b** Ag@GNRs. **c**HAA72175 UV–vis absorption spectra of GNRs and Ag@GNRs

Direct electrochemistry of Hb assembled on Ag@GNR-PSS-PDDA/GCE

Electrochemical behaviors of Hb on the modified electrodes were investigated by cyclic voltammetry (CV) with the results shown in Fig. 2a. No obvious redox peak can be observed at bare GCE (curve a), PDDA/GCE (curve b), PSS-PDDA/GCE (curve c) and Ag@GNR-PSS-PDDA/GCE (curve d), indicating no electroactive substances exist on the electrode surface. However, a couple of stable and well-defined redox peaks at −0.32 V and −0.40 V can be observed on Hb-Ag@GNR-PSS-PDDA/GCE (curve e), which is correspond with the characteristic of Hb-heme Fe(III)/Fe(II) reported by literature [40]. These results reveal that Ag@GNRs can provide a good microenvironment for Hb, so as to realize the direct electrochemical response and maintain the nature form of Hb.

Fig. 2b displays a series of cyclic voltammograms of Hb immobilized on Ag@GNR-PSS-PDDA/GCE in pH 7.0 phosphate buffer at the different scan rates. With an increasing scan rate ranging from 50 mV·s^{-1} to 600 mV·s^{-1}, the anodic and cathodic peak potentials of the Hb show a small shift and the redox peak currents increase linearly (inset in Fig. 2b), indicating a surface-controlled electrode process. According to Laviron eq. [41]:

$$I_p = \frac{n^2F^2A\Gamma\nu}{4RT} = \frac{\mathrm{nFQ\nu}}{4RT}$$

Where Γ represents the surface coverage of Hb (mol·cm^{-2}), Q is the total charge. I_p, T, F and R have the usual physical meaning. From the slope of the $I_p \propto \nu$, n is calculated to be 1.22, which demonstrates that the redox reaction of Hb at Ag@GNR-PSS-PDDA/GCE is a one-electron transfer process.

When $n\Delta E_p \le 200$ mV, electron transfer rate constant k_s can be calculated by the following formula [42]:

$$\log k_s = \alpha\log(1-\alpha) + (1-\alpha)\log\alpha - \log\frac{RT}{nF\nu} - \frac{\alpha(1-\alpha)nF\Delta E_p}{2.3RT}$$

Where α represents electron transfer constant, ΔE_p is peak-to-peak separation. When the scan rate sets as 100 mV·s^{-1}, k_s can be estimated to be 2.32 s^{-1}. The estimated value is in the controlled range of surface-controlled quasi-reversible process, and is larger than that of Hb assembled on AuNPs [43]. Such results reveal a reasonably fast electron transfer between the immobilized Hb and the underlying electrode.

The electrochemical behavior of Hb is significantly dependent on the solution pH. Therefore, the effect of solution pH was investigated by CV at different pH values of phosphate buffer and the results are shown in Fig. S2A and the corresponding plot of formal peak potential ($E^{0'}$) against pH is shown in Fig. S2B. The $E^{0'}$ was found to be linear with pH values over the range of 4.0–9.0 with a linear regression equation of $E^{0'}$(V) = 0.082–0.040 pH (R^2 = 0.984). The slope value of −40 mV· pH^{-1} is smaller than the theoretically expected value of −57.6 mV· pH^{-1} for a single-proton coupled to the reversible one-electron transfer at 18 °C [44]. It may be due to the influence of the protonization of ligands to the heme iron and amino acids around the heme [45]. The influence of temperature of phosphate buffer on the cyclic voltammograms of Hb-Ag@GNR-PSS-PDDA/GCE is shown in Fig. S3A. The details discussed in ESM indicate that Hb still maintain good biological activity with the temperature in the range of 15–45 °C.

Electrocatalytic behavior of Hb-Ag@GNR-PSS-PDDA/GCE

To explore the applicability of the Hb-Ag@GNR-PSS-PDDA/GCE for TCA biosensing, CVs were carried out

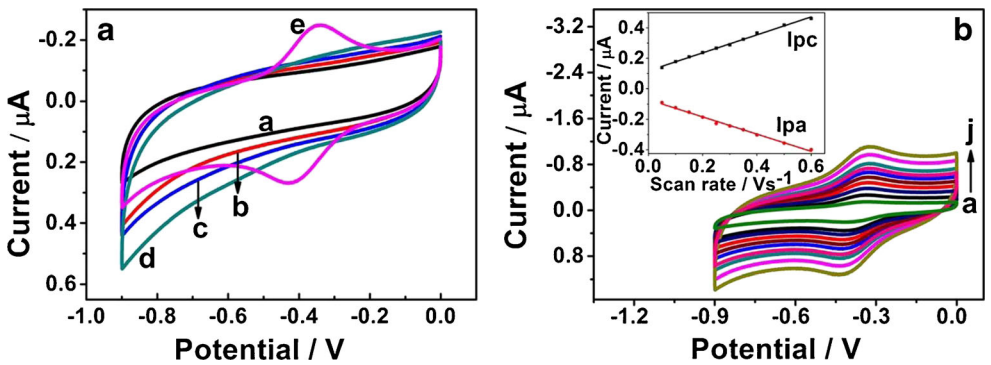

Fig. 2 **a** Cyclic voltammograms of (**a**) GCE, (**b**) PDDA/GCE, (**c**) PSS-PDDA/GCE, (**d**) Ag@GNR-PSS-PDDA/GCE and (**e**) Hb-Ag@GNR-PSS-PDDA/GCE in 0.1 M pH 7.0 phosphate buffer. Scan rate: 100 mV·s^{-1}. **b** Cyclic voltammograms on Hb-Ag@GNR-PSS-PDDA/GCE in pH 7.0 phosphate buffer at scan rates of 50, 100, 150, 200, 250, 300, 350, 400, 500 and 600 mV·s^{-1} (from a to j). Inset: The linear relationship between the redox current (I_p) and the scan rate (ν)

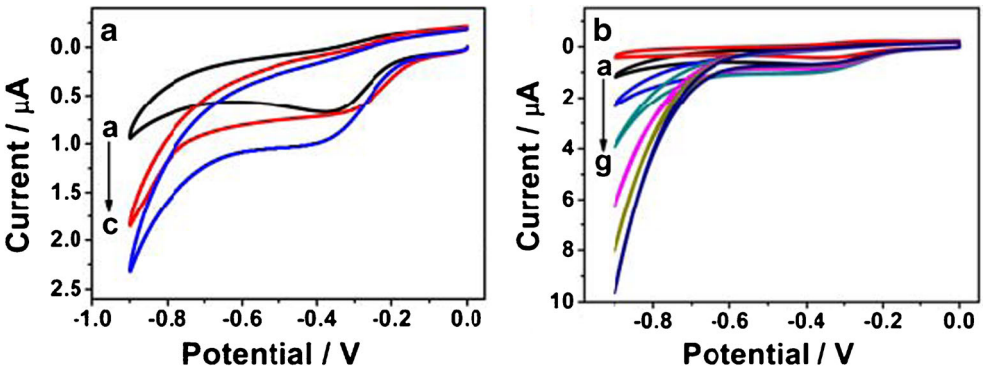

Fig. 3 **a** Cyclic voltammograms of (**a**) Hb-GNR-PSS-PDDA/GCE, (**b**) Hb-AgNP-PSS-PDDA/GCE and (**c**) Hb-Ag@GNR-PSS-PDDA/GCE in pH 4.0 phosphate buffer containing 2.0 μM TCA. Scan rate: 100 $mV \cdot s^{-1}$. **b** Cyclic voltammograms of Hb-Ag@GNR-PSS-PDDA/GCE in pH 4.0 phosphate buffer containing 0, 1.3, 2.0, 2.7, 3.4, 5.3 and 8.7 μM TCA (*curves* **a**–**g**)

to demonstrate the electrochemical reduction of TCA at the modified electrode in pH 4.0 phosphate buffer. The electrochemical reduction of TCA can be promoted in acid medium due to a large number of hydrogen ions on the surface of modified electrode. Meanwhile, because the isoelectric point of Hb is about 6.8 [46], the Hb-Ag@GNR-PSS-PDDA/GCE would be positively charged at pH 4.0. Due to the anionic property of TCA, the acidic Hb-Ag@GNR-PSS-PDDA/GCE surface seems profitable for the adsorption of TCA. Therefore, the acid medium can promote the electrocatalytic activity of TCA.

As shown in Fig. 3a, the electrochemical response of TCA at Hb-Ag@GNR-PSS-PDDA/GCE was investigated using CV. When 2.0 μM TCA was added into the phosphate buffer, a great increase of the reduction peak was observed at about −0.4 V with the simultaneous disappearance of the oxidation peak. In addition, compared with the single nanoparticles modified electrode, it can be clearly seen that Hb-Ag@GNR-PSS-PDDA/GCE exhibits more sensitive response to TCA. It reveals that Ag@GNRs can accelerate the electron transfer between TCA and the modified electrode owing to the synergistic effect of AgNPs and GNRs together. Therefore, the modified electrode based on Ag@GNRs can be used as a good electrochemical platform for determining TCA.

Fig. 3b shows the CVs of Hb-Ag@GNR-PSS-PDDA/GCE in pH 4.0 phosphate buffer containing different concentrations of TCA. When the concentration of TCA increased, the reduction peak current at −0.40 V increased gradually with the disappearance of the oxidation peak current which demonstrates the typical characteristic of the electrocatalytic reaction. Electrocatalytic reduction mechanism of TCA by the Hb modified electrode can be expressed with the following Eqs. [47]:

$$\mathrm{HbhemeFe(III)} + \mathrm{e} \rightarrow \mathrm{HbhemeFe(II)}$$

$$2\mathrm{HbhemeFe(II)} + \mathrm{CCl_3COOH} + \mathrm{H^+} + \mathrm{e} \rightarrow 2\mathrm{HbhemeFe(III)} + \mathrm{Cl_2CHCOOH} + \mathrm{Cl^-}$$

Fig. 4 shows the typical amperometric response of TCA on the Hb modified electrode at an applied potential of −0.4 V. The current increases with each increment of TCA within a linear range from 0.16 μM to 1.7 μM. The linear regression equation is i(A) =0.00655 [TCA] (M) + 8.77 × 10^{-8} (R^2 = 0.9975). The detection limit is 0.12 μM (S/N = 3). Electrocatalytic activity of Hb-Ag@GNR-PSS-PDDA/GCE and other sensors toward TCA are compared in Table 1. From Table 1, we can see that the detection potential is relatively low and thus the oxidation of common interferents can hardly happen at such negative potential. Meanwhile, compared with other reports, the detection limit is lower than that of some reported values such as CTS/Hb/Ag/GR/CILE (42 mM) and CTS/Hb-Fe_3O_4/GCE (33 μM). However, the linear range of this biosensor is narrower than other reported methods [48, 49].

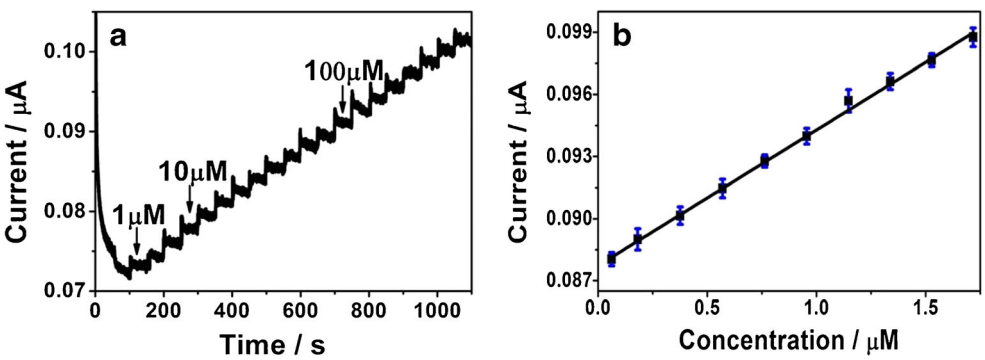

Fig. 4 **a** The amperometric response of HbAg@GNR-PSS-PDDA/GCE upon successive addition of 10 μL TCA to pH 4.0 phosphate buffer with stirring. Working potential: −0.4 V (vs. SCE) **b** Linear relationship of electrocatalytic current vs. concentration of TCA

Table 1 Comparison of the analytical performance for TCA with others

Modified electrode	Method	Line range (M)	LOD (M)	Potential (V)	Sample	Reference
AFIL-LDH-Hbcop/GCE	CV	$0.8 \times 10^{-3} \sim 4.3 \times 10^{-1}$	1.9×10^{-4}	−0.28	Tap water	[24]
SWNTs-Hb microbelts/GCE	CV	$1.2 \times 10^{-5} \sim 1.1 \times 10^{-3}$	2.4×10^{-6}	−0.40	Tap water	[25]
CTS/Hb-Fe_3O_4/GCE	CV	$2.4 \times 10^{-3} \sim 2.0 \times 10^{-2}$	3.3×10^{-5}	−0.36	-	[26]
Hb/Nafion/GR-TiO_2/CILE	CV	$0.6 \times 10^{-3} \sim 2.1 \times 10^{-2}$	2.2×10^{-7}	−0.32	-	[27]
Hb/CTS/GR-LDH/CILE	CV	$1.6 \times 10^{-3} \sim 2.5 \times 10^{-2}$	5.3×10^{-7}	−0.30	Laboratory water	[28]
Hb/CS/Au@Fe_3O_4/GCE	i-t	$1.6 \times 10^{-6} \sim 4.8 \times 10^{-3}$	1.0×10^{-6}	−0.20	-	[29]
CTS/Hb/Ag/GR/CILE	CV	$8.0 \times 10^{-4} \sim 2.2 \times 10^{-2}$	4.2×10^{-4}	−0.22	-	[52]
Mb/GR-IL/CILE	CV	$2.0 \times 10^{-3} \sim 1.6 \times 10^{-2}$	5.8×10^{-4}	−0.56	-	[53]
MWCNTs/Pc/Fe(II)	CV	$8.0 \times 10^{-6} \sim 2.0 \times 10^{-3}$	2.0×10^{-6}	−0.40	Tap water	[54]
Hb-Ag@GNRs-PSS-PDDA/GCE	i-t	$1.6 \times 10^{-7} \sim 1.7 \times 10^{-6}$	1.2×10^{-7}	−0.40	Laboratory water	This work

CTS chitosan, *GR* graphene, *LDH* layered double hydroxides, *IL* ionic liquids, *CILE* Carbon ionic liquid electrode, *MWCNTs* multiwalled carbon nanotubes, *Pc* phthalocyanine, *i-t* amperometric i-t curve, *AFIL* amino functionalized ionic liquid, *SWNTs* Single-walled carbon nanotubes, *cop* coprecipitation

The apparent Michaelis-Menten constant (K_m), which is an indication of the enzyme-substrate reaction kinetics, is calculated by the Lineweaver-Burk eq. [50]:

$$\frac{1}{I_{SS}} = \frac{Km}{I_{max}} \cdot \frac{1}{C} + \frac{1}{I_{max}}$$

Where, I_{ss} is the steady-state current after the addition of substrate, C is the bulk concentration of substrate, and I_{max} is the maximum current under saturated substrate conditions and measured as 0.102 μA. K_m value for Hb-Ag@GNR-PSS-PDDA modified electrode was estimated to be 0.996 μM. The lower value of K_m was smaller than that of Hb immobilized on CTS/NG/Hb film modified CILE (4.3 mM) [51] and CTS/Hb/Ag/GR modified CILE (10.2 mM) [52].

Interference studies

The potential interferences to the determination of 1.0 μM TCA were investigated on Hb-Ag@GNR-PSS-PDDA/GCE under the optimized conditions. The changes of the peak current were calculated with the results summarized in Table 2. It can be seen that 100 times of the TCA comcentration of Ba^{2+}, Ca^{2+}, Mg^{2+}, Zn^{2+}, Na^+, K^+, Cu^{2+}, SO_4^{2-}, $NO_3^-$and Cl^- did not interfere with the electrochemical responses of TCA. Other species such as dichloroacetic acid and monochloroacetic acid can be present at less than 30 times of the TCA concentration. In addition, the same concentration of Pb^{2+} can be tolerated with the changes less than ±5%. The only serious interference was H_2O_2. The same effect has been observed earlier and has been the subject of many studies [53, 55].

Determination of TCA in laboratory water samples

This electrochemical method was used to detect the TCA content in laboratory water samples and the results were listed in Table 3. The accuracy of the method was evaluated by the recovery test which was implemented by the standard addition method. The recoveries are ranged from 92.71% to 107.50%, which indicate that this sensor exhibits an acceptable accuracy for the analysis of TCA in laboratory water samples.

Table 2 Influence of coexisting substances on the detection of 1.0 μM TCA (n = 3)

Coexistent substance	Concentration (μM)	RSD (%)	Coexistent substance	Concentration (μM)	RSD (%)
Ba^{2+}	100.0	+4.39	SO_4^{2-}	100.0	+2.85
Ca^{2+}	100.0	+2.80	NO_3^-	100.0	+2.94
Mg^{2+}	100.0	+3.52	Cl^-	100.0	+2.63
Zn^{2+}	100.0	+3.26	dichloroacetic acid	30.0	+4.25
Na^+	100.0	−2.33	monochloroacetic acid	30.0	+3.17
K^+	100.0	−3.42	Pb^{2+}	1.0	+3.97
Cu^{2+}	100.0	+4.13	H_2O_2	1.0	+12.43

Table 3 Analysis of TCA in laboratory water samples (n = 3)

Sample	Labeled (μM)	Detected (μM)	Added (μM)	Found (μM)	Recovery (%)	RSD (%)
Water	0	0	0.40	0.39	98.13	3.82
	0	0	0.80	0.86	107.50	5.45
	0	0	1.20	1.11	92.71	7.05

Stability and reproducibility of Hb-Ag@GNR-PSS-PDDA/GCE

We studied the stability of the biosensor by storing it at 4 °C in pH 4.0 phosphate buffer and measured intermittently. A week later the current response of the biosensor still retained 95% of the initial value. The good stability of the biosensor can be ascribed to the Ag@GNR-nanocomposite, which provides a favorable microenviroment for immobilizing Hb effectively and keep its bioactivity on the electrode surface. The repeatability was also investigated for 6 successive measurements at TCA concentration of 1.0 μM and it exhibited a good result with the RSD of 4.2%.

Conclusions

In summary, the Ag@GNRs with the shell-core structure was successfully synthesized and used as an effective electrocatalyst for fabrication of the Hb modified electrode. Hb on the Ag@GNR-film keeps its natural structure and bioactivity and the fast direct electron transfer is realized. The electrochemical studies suggest that the resulting electrode exhibits good electrocatalytic activity to the reduction of TCA. The amperometric detection of TCA exhibits a wide linear concentration range and a low detection limit. Therefore, the application of Ag@GNR-composite can afford an effective platform for the immobilization of Hb and the construction of biosensors. The biosensor possesses good stability and reproducibility, which would be capable of being a potential biosensing platform in the electroanalysis and electrocatalysis.

Acknowledgements This work was financially supported by the National Natural Science Foundation of China (21375066 and 21475070), the Natural Science Foundation of Jiangsu Province (BK20151267), the Qing Lan Project of Jiangsu Province, the Priority Academic Program Development of Jiangsu Higher Education Institutions (PAPD) and the Application Research Item of Nantong City (MS12015046).

Compliance with ethical standards The author(s) declare that they have no competing interests.

References

1. Mai Z, Zhao X, Dai Z, Zou X (2010) Direct electrochemistry of hemoglobin adsorbed on self-assembled monolayers with different head groups or chain length. Talanta 81:167–175
2. Saadati S, Salimia A, Hallaj R, Rostami A (2014) Direct electron transfer and electrocatalytic properties of immobilized hemoglobin onto glassy carbon electrode modified with ionic-liquid/titanium-nitride nanoparticles: application to nitrite detection. Sensor Actuat B-Chem 191:625–633
3. Palanisamy S, Wang YT, Chen SM, Thirumalraj B, Lou BS (2016) Direct electrochemistry of immobilized hemoglobin and sensing of bromate at a glassy carbon electrode modified with graphene and β-cyclodextrin. Microchim Acta 183:1953–1961
4. Wu YF, Xue P, Kang YJ, Hui KM (2013) Highly specific and ultrasensitive graphene-enhanced electrochemical detection of low-abundance tumor cells using silica nanoparticles coated with antibody-conjugated quantum dots. Anal Chem 85:3166–3173
5. Huang QT, Zhang HQ, Hu SR, Li FM, Weng W, Chen JH, Wang QX, He YS, Zhang WX, Bao XX (2014) A sensitive and reliable dopamine biosensor was developed based on the Au@carbon dots-chitosan composite film. Biosens Bioelectron 52:277–280
6. Zang S, Liu YJ, Lin MH, Kang JL, Sun YM, Lei HT (2013a) A dual amplified electrochemical immunosensor for ofloxacin: polypyrrole film-Au nanocluster as the matrix and multi-enzyme-antibody functionalized gold nanorod as the label. Electrochim Acta 90:246–253
7. Navaei A, Saini H, Christenson W, Sullivan RT, Ros R, Nikkhah M (2016) Gold nanorod-incorporated gelatin-based conductive hydrogels for engineering cardiac tissue constructs. Acta Biomater 41:133–146
8. Khlebtsov BN, Khanadeev VA, Ye J, Sukhorukov GB, Khlebtsov NG (2014) Overgrowth of gold nanorods by using a binary surfactant mixture. Langmuir 30:1696–1703
9. Komathi S, Gopalan AI, Kim SK, Anand GS, Lee KP (2013) Fabrication of horseradish peroxidase immobilized poly(n-[3-(trimethoxy silyl)propyl]aniline) gold nanorods film modified electrode and electrochemical hydrogen peroxide sensing. Electrochim Acta 92:71–78
10. Bai W, Huang H, Li Y, Zhang H, Liang B, Guo R (2014a) Direct preparation of well-dispersed graphene/gold nanorod composites and their application in electrochemical sensors for determination of ractopamine. Electrochim Acta 117:322–328
11. Shakoori Z, Salimian S, Kharrazi S, Adabi M, Saber R (2015) Electrochemical DNA biosensor based on gold nanorods for detecting hepatitis B virus. Anal Bioanal Chem 407:455–461
12. Azimzadeh M, Rahaie M, Nasirizadeh N, Ashtari K, Naderi-Manesh H (2016) An electrochemical nanobiosensor for plasma miRNA-155, based on graphene oxide and gold nanorod, for early detection of breast cancer. Biosens Bioelectron 77:99–106
13. Yang XJ, Wang YH, Liu YW, Jiang XE (2013) A sensitive hydrogen peroxide and glucose biosensor based on gold/silver core–shell nanorods. Electrochim Acta 108:39–44
14. Zhang Y, Lu F, Yan Z, Wu D, Ma H, Du B (2015a) Electrochemiluminescence immunosensing strategy based on the use of Au@Ag nanorods as a peroxidase mimic and NH_4CoPO_4 as a supercapacitive supporter: application to the determination of carcinoembryonic antigen. Microchim Acta 182:1–9
15. Tang LJ, Li S, Han F, Liu LQ, Xu LG, Ma W, Kuang H, Li AK, Wang LB, Xu CL (2015) SERS-active Au@Ag nanorod dimers for ultrasensitive dopamine detection. Biosens Bioelectron 71:7–12
16. Sun JD, Ji J, Sun YQ, Abdalhai MH, Zhang YZ, Sun XL (2015) DNA biosensor-based on fluorescence detection of *E. coli* O157:H7 by Au@Ag nanorods. Biosens Bioelectron 70:239–245

17. Zhang HF, Ning DL, Ma L, Zheng JB (2016) Silver deposition directed by self-assembled gold nanorods for amplified electrochemical immunoassay. Anal Chim Acta 902:82–88
18. Bull RJ, Sanchez IM, Nelson MA, Larson JL, Lansing AJ (1990) Liver tumor induction in B6C3F1 mice by dichloroacetate and trichloroacetate. Toxicology 63:341–359
19. Dojlido J, Zbieć E, Świetlik R (1999) Formation of the haloacetic acids during ozonation and chlorination of water in Warsaw waterworks (Poland). Water Res 33:3111–3118
20. Ferreira AMC, Laespada MEF, Pavon JLP, Cordero BM (2013) In situ derivatization coupled to microextraction by packed sorbent and gas chromatography for the automated determination of haloacetic acids in chlorinated water. J Chromatogr A 1318:35–42
21. Prieto-Blanco MC, Alpendurada MF, López-Mahía P, Muniategui-Lorenzo S, Prada-Rodríguez D, Machado S, Gonçalves C (2012) Improving methodological aspects of the analysis of five regulated haloacetic acids in water samples by solid-phase extraction, ion-pair liquid chromatography and electrospray tandem mass spectrometry. Talanta 94:90–98
22. Boysen G (2009) Liquid chromatography electrospray ionization tandem mass spectrometry analysis method for simultaneous detection of trichloroacetic acid, dichloroacetic acid, S-(1,2-dichlorovinyl)glutathione and S-(1,2-dichlorovinyl)-L-cysteine. Toxicology 262:230–238
23. Dai H, Xu H, Wu X, Lin Y, Wei M, Chen G (2010) Electrochemical behavior of thionine at titanate nanotubes-based modified electrode: a sensing platform for the detection of trichloroacetic acid. Talanta 81:1461–1466
24. Zhan T, Wang X, Zhang Y, Song Y, Liu X, Xu J (2015) Direct electrochemistry and electrocatalysis of hemoglobin immobilized in layered double hydroxides modified with amino functionalized ionic liquid through coprecipitation technique. Sensor Actuat B-Chem 220:1232–1240
25. Ding Y, Wang Y, Lei Y (2010) Direct electrochemistry and electrocatalysis of novel single-walled carbon nanotubes–hemoglobin composite microbelts—towards the development of sensitive and mediator-free biosensor. Biosens Bioelectron 26:390–397
26. Sun W, Sun ZL, Zhang LQ, Qi XW, Li GJ, Wu J, Wang M (2013a) Application of Fe_3O_4 mesoporous sphere modified carbon ionic liquid electrode as electrochemical hemoglobin biosensor. Colloid Surface B 101:177–182
27. Sun W, Guo YQ, Ju XM, Zhang YY, Wang XZ, Sun ZF (2013b) Direct electrochemistry of hemoglobin on graphene and titanium dioxide nanorods composite modified electrode and its electrocatalysis. Biosens Bioelectron 42:207–213
28. Sun W, Guo YQ, Lu YP, Hu AH, Shi F, Li TT, Sun ZF (2013c) Electrochemical biosensor based on graphene, Mg_2Al layered double hydroxide and hemoglobin composite. Electrochim Acta 91:130–136
29. Liu Y, Han T, Chen C, Bao N, Yu CM, Gu HY (2011) A novel platform of hemoglobin on core-shell structurally Fe_3O_4@Au nanoparticles and its direct electrochemistry. Electrochim Acta 56:3238–3247
30. Ye XC, Zheng C, Chen J, Gao YZ, Murray CB (2013) Using binary surfactant mixtures to simultaneously improve the dimensional tunability and monodispersity in the seeded growth of gold nanorods. Nano Lett 13:765–771
31. Casas J, Venkataramasubramani M, Wang YY, Tang L (2013) Replacement of cetyltrimethylammoniumbromide bilayer on gold nanorod by alkanethiol crosslinker for enhanced plasmon resonance sensitivity. Biosens Bioelectron 49:525–530
32. Meng J, Ji YL, Liu J, Cheng XL, Guo H, Zhang WQ, Wu XC, Xu HY (2014) Using gold nanorods core/silver shell nanostructures as model material to probe biodistribution and toxic effects of silver nanoparticles in mice. Nanotoxicology 8:686–696
33. Wang XK, Chen L, Chen LX (2014) Colorimetric determination of copper ions based on the catalytic leaching of silver from the shell of silver-coated gold nanorods. Microchim Acta 181:105–110
34. Yu C, Zhou X, Gu H (2010) Immobilization, direct electrochemistry and electrocatalysis of hemoglobin on colloidal silver nanoparticles-chitosan film. Electrochim Acta 55:8738–8743
35. Feng Q, Liu K, Fu J, Zhang Y, Zheng Z, Wang C (2012) Direct electrochemistry of hemoglobin based on nano-composite film of gold nanopaticles and poly (diallyldimethylammonium chloride) functionalized graphene. Electrochim Acta 60:304–308
36. Fu Q, Liu HL, Wu Z, Liu A, Yao C, Li X (2015) Rough surface Au@Ag core–shell nanoparticles to fabricating high sensitivity SERS immunochromatographic sensors. J Nanobiotechnol 13:1–9
37. Bai T, Sun J, Che R, Xu L, Yin C, Guo Z (2014b) Controllable preparation of core-shell Au-Ag nanoshuttles with improved refractive index sensitivity and SERS activity. ASC Appl Mater Inter 6:3331–3340
38. Jayabal S, Ramaraj R (2014) Bimetallic Au/Ag nanorods embedded in functionalized silicate sol–gel matrix as an efficient catalyst for nitrobenzene reduction. Appl Catal A-Gen 470:369–375
39. Zhang S, Han L, Hou C, Li C, Lang Q, Han L (2015b) Novel glucose sensor with Au@Ag heterogeneous nanorods based on electrocatalytic reduction of hydrogen peroxide at negative potential. J Electroanal Chem 742:84–89
40. Royo B, Sosna M, Asensio AC, Moran JF, Ferapontova EE (2013) Direct electrochemistry and environmental sensing of rice hemoglobin immobilized at graphite electrodes. J Electroanal Chem 704:67–74
41. Laviron E (1979a) The use of linear potential sweep voltammetry and of a.C. Voltammetry for the study of the surface electrochemical reaction of strongly adsorbed systems and of redox modified electrodes. J Electroanal Chem 100:263–270
42. Laviron E (1979b) General expression of the linear potential sweep voltammogram in the case of diffusionless electrochemical systems. J Electroanal Chem 101:19–28
43. Liu Y, Jiang QY, Lu SY, Zhang Y (2009) Immobilization of hemoglobin on the gold colloid modified pretreated glassy carbon electrode for preparing a novel hydrogen peroxide biosensor. Appl Biochem Biotech 152:418–427
44. Bond AM (1980) Modern Polarographic methods in analytical chemistry. Marcel Dekker, New York, pp p29–p30
45. Yamazaki I, Araiso T, Hayashi Y, Yamada H, Makino R (1978) Analysis of acid-base properties of peroxidase and myoglobin. Adv Biophys 11:249–281
46. Herzog G, Kam V, Arrigan DWM (2008) Electrochemical behaviour of haemoglobin at the liquid/liquid interface. Electrochim Acta 53:7204–7209
47. Shie JW, Yogeswaran U, Chen SM (2009) Haemoglobin immobilized on nafion modified multi-walled carbon nanotubes for O_2, H_2O_2 and CCl_3COOH sensors. Talanta 78:896–902
48. Zhan T, Wang X, Li X, Song Y, Hou W (2016) Hemoglobin immobilized in exfoliated Co_2Al LDH-graphene nanocomposite film: direct electrochemistry and electrocatalysis toward trichloroacetic acid. Sensor Actuat B-Chem 228:101–108
49. Zhu Z, Qu L, Niu Q, Zeng Y, Sun W, Huang X (2011) Urchinlike MnO_2, nanoparticles for the direct electrochemistry of hemoglobin with carbon ionic liquid electrode. Biosens Bioelectron 26:2119–2124
50. Kamin RA, Wilson GS (1980) Rotating ring-disk enzyme electrode for biocatalysis kinetic studies and characterization of the immobilized enzyme layer. Anal Chem 52:1198–1205
51. Sun W, Dong L, Deng Y, Yu J, Wang W, Zhu Q (2014) Application of N-doped graphene modified carbon ionic liquid electrode for direct electrochemistry of hemoglobin. Mat Sci Eng C-Mater 39:86–91

52. Sun W, Zhang YY, Wang XZ, Ju XM, Wang D, Wu J, Sun ZF (2012) Electrodeposited graphene and silver nanoparticles modified electrode for direct electrochemistry and electrocatalysis of hemoglobin. Electroanalysis 24:1973–1979
53. Ruan CX, Li TT, Niu QJ, Lu M, Lou J, Gao WM, Sun W (2012) Electrochemical myoglobin biosensor based on graphene-ionic liquid-chitosan bionanocomposites: direct electrochemistry and electrocatalysis. Electrochim Acta 64: 183–189
54. Kurd M, Salimi A, Hallaj R (2013) Highly sensitive amperometric sensor for micromolar detection of trichloroacetic acid based on multiwalled carbon nanotubes and Fe(II)-phtalocyanine modified glassy carbon electrode. Mat Sci Eng C-Mater 33:1720–1726
55. Sun W, Cao L, Deng Y, Gong S, Shi F, Li G (2013d) Direct electrochemistry with enhanced electrocatalytic activity of hemoglobin in hybrid modified electrodes composed of graphene and multiwalled carbon nanotubes. Anal Chim Acta 781:41–47